2-8-2017

Half-metallic magnetism in Ti3Co5-xFexB2

Rohit Pathak
Indian Institute of Technology

Imran Ahamed
Indian Institute of Technology

W. Y. Zhang
University of Nebraska-Lincoln

Shah Vallopilly
University of Nebraska-Lincoln

D. J. Sellmyer
University of Nebraska-Lincoln, dsellmyer@unl.edu

See next page for additional authors

Half-metallic magnetism in $Ti_3Co_{5-x}Fe_xB_2$

Rohit Pathak,[1] Imran Ahamed,[1] W. Y. Zhang,[2] Shah Vallopilly,[2]
D. J. Sellmyer,[2] Ralph Skomski,[2] and Arti Kashyap[1]
[1]*School of Basic Sciences, Indian Institute of Technology, Mandi 175001, Himachal Pradesh, India*
[2]*Nebraska Center for Materials and Nanoscience and Department of Physics and Astronomy, University of Nebraska, Lincoln, Nebraska 68588, USA*

(Presented 1 November 2016; received 23 September 2016; accepted 12 November 2016; published online 8 February 2017)

Bulk alloys and thin films of Fe-substituted $Ti_3Co_5B_2$ have been investigated by first-principle density-functional calculations. The series, which is of interest in the context of alnico magnetism and spin electronics, has been experimentally realized in nanostructures but not in the bulk. Our bulk calculations predict paramagnetism for $Ti_3Co_5B_2$, $Ti_3Co_4FeB_2$ and $Ti_3CoFe_4B_2$, whereas $Ti_3Fe_5B_2$ is predicted to be ferromagnetic. The thin films are all ferromagnetic, indicating that moment formation may be facilitated at nanostructural grain boundaries. One member of the thin-film series, namely $Ti_3CoFe_4B_2$, is half-metallic and exhibits perpendicular easy-axis magnetic anisotropy. The half-metallicity reflects the hybridization of the Ti, Fe and Co 3*d* orbitals, which causes a band gap in minority spin channel, and the limited equilibrium solubility of Fe in bulk $Ti_3Co_5B_2$ may be linked to the emerging half-metallicity due to Fe substitution. [http://dx.doi.org/10.1063/1.4976302]

I. INTRODUCTION

The tetragonal intermetallic compound $Ti_3Co_5B_2$[1] has long been known to be non-magnetic (Pauli paramagnetic), but recent experimental research has found that Fe substitution makes the alloy ferromagnetic.[2] This is important in two contexts. First, the melt-spun samples considered in Ref. 2 form part of ongoing efforts to create magnetocrystalline anisotropy in alnico-type permanent magnets.[3,4] The tetragonal crystal structure of the alloy supports uniaxial anisotropy, which is much stronger than the cubic anisotropy of the main magnetic bcc-type Fe-Co phase and may complement the shape anisotropy of the material. Any additional magnetocrystalline anisotropy would substantially enhance the coercivity, which is the performance bottleneck in an otherwise very good permanent-magnet material. Second, the search for new magnetic materials with uniaxial anisotropy is a key aspect of the ongoing development of spin-electronics materials.[5–8] Among the desired properties for spin-electronics applications are a high spin polarization at the Fermi level, ideally half-metallicity,[9–17] and some noncubic anisotropy.[18–21]

However, the formation of the Ti-Co-Fe-B alloy is limited to nanostructured magnets produced by melt-spinning, and our attempts to produce the corresponding bulk phase by arc melting have been unsuccessful. In other words, experiment indicates that the equilibrium solubility of Fe in bulk $Ti_3Co_5B_2$ is very limited, and no theoretical investigations of Fe-substituted $Ti_3Co_5B_2$ have been published so far. In this paper, we consider thin-film and bulk $Ti_3Co_5B_2$, $Ti_3Co_4FeB_2$, $Ti_3CoFe_4B_2$ and $Ti_3Fe_5B_2$, calculating the electronic structure, the magnetic moment, and the magnetocrystalline anisotropy.

II. METHODS AND CALCULATION

This section outlines the considered bulk and thin-film structures of $Ti_3Co_{5-x}Fe_xB_2$ (x = 0, 1, 4, 5) and methodical details of the first-principle calculation.

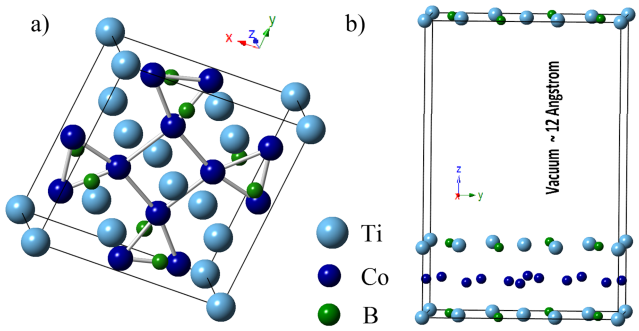

FIG. 1. Crystal structures (unit cells) of the considered $Ti_3(Co, Fe)_5B_2$ materials: (a) bulk and (b) thin film along (001) direction.

A. Structural details

Figure 1(a) show the bulk crystal structure of the parent compound $Ti_3Co_5B_2$ (space group P4/mbm, no. 127),[1] which has a stacking of alternating layers of Ti_3B_2 and Co_5. The unit cell contains 20 atoms with 4 different sites, namely 8j, 2c, 2a and 4g, where the Ti atoms occupy 4g and 2a sites, the Co atoms occupy the 2c and 8j sites, and the B atoms occupy the 2a sites. The Wyckoff positions for Ti1, Ti2, Co1, Co2 and B are (0,0,0), (0.327, 0.827, 0), (0, 0.5, 0.5), (0.222, 0.068, 0.5) and (0.115, 0.615, 0), respectively. The unit cell is compatible with several ordered compounds ($Ti_3Co_5B_2$, $Ti_3Co_4FeB_2$, $Ti_3CoFe_4B_2$ and $Ti_3Fe_5B_2$) and with many chemically disordered alloys.

Thin films of three atomic layers, Fig. 1(b), have been created for all the four members of the series, using the supercell method along *c*-axis direction. The compositions of the thin films non-stoichiometric but Co- and Fe-lean compared to the corresponding bulk alloys. The atomic layers have surface-to-surface spacings of 12 Å, to ensure that the tails of the atomic wave functions do not introduce a hybridization error by hybridizing through the vacuum.

B. Density-functional calculations

The $Ti_3Co_{5-x}Fe_xB_2$ bulk and thin-film structures were investigated using first principle calculations, employing the generalized gradient approximation (GGA) for exchange and correlations.[22] The calculations are based on the projector augmented wave (PAW)[23] implemented in the Vienna Ab-initio Simulation Package (VASP).[24] Experimental lattice parameters[1] were used for parent system $Ti_3Co_5B_2$, namely $a = 8.489$ □ and $c = 3.038$ □. The Brillion-zone integration is performed using a 15 × 15 × 45 Monkhorst-Pack[25] *k*-point grid for bulk and a 15 × 15 × 1 Monkhorst-Pack k-point grid for thin films made in *z*-direction. To represent the electronic wave functions, we have used an energy cutoff of 600 eV and to ensure well-defined *k*-states, we have performed supercell calculations where the particles are periodically repeated in space. The magnetic anisotropy and orbital moments are relativistic effects and therefore involve the spin-orbit coupling, which has been implemented by Kresse and Lebacq in VASP. We have performed volume optimization and ionic relaxation for the other three members of the series namely $Ti_3Co_4FeB_2$, $Ti_3CoFe_4B_2$ and $Ti_3Fe_5B_2$ to get the optimized lattice parameters.

III. RESULTS AND DISCUSSION

We have systematically studied $Ti_3Co_{5-x}Fe_xB_2$ series of compounds in bulk as well as in thin film. Subsection III A discusses results for bulk alloys and Subsection III B discusses results for thin films.

A. Bulk calculations

We have performed volume optimization and ionic relaxation to get optimized lattice parameters for $Ti_3Co_4FeB_2$, $Ti_3CoFe_4B_2$ and $Ti_3Fe_5B_2$, whereas for the parent alloy $Ti_3Co_5B_2$ we merely

TABLE I. Lattice parameters and magnetic order for all four bulk compounds.

Compound	Lattice Parameter (Å)	Magnetic Order
$Ti_3Co_5B_2$	$a = b = 8.489$, $c = 3.038$	Paramagnetic
$Ti_3Co_4FeB_2$	$a = b = 8.469$, $c = 3.018$	Paramagnetic
$Ti_3CoFe_4B_2$	$a = b = 8.618$, $c = 2.899$	Paramagnetic
$Ti_3Fe_5B_2$	$a = b = 8.633$, $c = 2.896$	Ferromagnetic

performed relaxation for the experimental lattice parameters.[1] Table I summarizes the optimized lattice parameters for all four compounds.

Our calculations show that only one member of the bulk series, namely the fully substituted alloy $Ti_3Fe_5B_2$, is ferromagnetic. The other compounds, where Co is only partially replaced by Fe, are paramagnetic. In $Ti_3Fe_5B_2$, the magnetic moment originates from the Fe 3*d* electrons, as we can see from Fig. 2, and the magnetic moment is 0.37 μ_B per Fe atom.

B. Thin film calculations

We have performed ionic relaxation in the supercell, keeping the volume and shape fixed, in order to find the optimized lattice parameters for our thin-film calculations. After ionic relaxation, the distance between bottom two layers remain same as of bulk system whereas the distance between top two layers gets increased by respective amounts of 0.086 Å, 0.077 Å, 0.021 Å, and 0.025 Å for $Ti_3Co_5B_2$, $Ti_3Co_4FeB_2$, $Ti_3CoFe_4B_2$, and $Ti_3Fe_5B_2$ compared to the bulk alloys. All films are ferromagnetic; Table II shows the lattice parameters and the magnetic moments per transition metal.

The ferromagnetism of the members of the thin-film series is clearly visible in the total densities of states (DOS), which are shown in Fig. 3. In each thin film, the surface Ti atoms contribute to the magnetic moment of the system, that is, the films exhibit surface Ti magnetism. The reason for the uncompensated Ti surface spins is that the vacuum causes a reduced hybridization of the 3*d* orbitals along the *c*-axis. The Ti surface magnetism is intriguing in the context of possible Ti terminations at interfaces in multilayers and nanogranular magnets.

Our results also support the suggestion by Zhang *et al.*[2] that coercivity enhancement in alnico magnets is possible due to presence of tetragonal $Ti_3(Fe,Co)_5B_2$ phase. In fact, their melt-spun samples contain many interfaces and are therefore closer to thin films than to bulk crystalline materials.

Interestingly, one member of the thin-film series, namely $Ti_3CoFe_4B_2$, is predicted to be half-metallic, adding a new compound to the dictionary of half-metallic compounds. The half-metallicity reflects the hybridization of 3*d* orbitals of the transition metals Ti, Fe and Co present in the compound, which causes a band gap in minority spin channel, as we can see the partial density of states in Fig. 4. The half-metallicity is essentially a band-filling effect, because Fe has one less electron per atom than Co, shifting the Fermi level down to the minority band gap. The tendency towards a half-metallic gap may be one reason for the limited equilibrium solubility of Fe in bulk $Ti_3Co_5B_2$, because the opening of a gap affects the energetics as a function of the number of *d* electrons. However, this question requires further research.

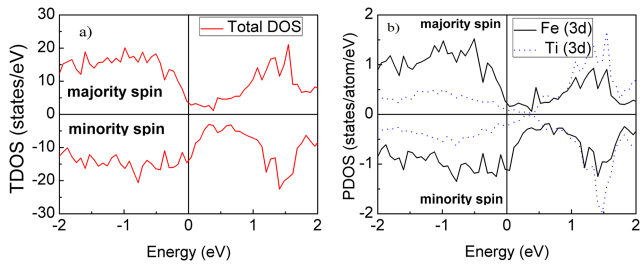

FIG. 2. Densities of states (DOS) in bulk $Ti_3Fe_5B_2$: (a) total DOS and (b) partial DOS.

TABLE II. Lattice parameters and magnetic moments per thin-film super cell.

Compound	Lattice Parameter (Å)	Magnetic Moment (μ_B/surface Ti atom)
$Ti_3Co_5B_2$	$a = b = 8.469$, $c = 15.090$	0.635
$Ti_3Co_4FeB_2$	$a = b = 8.469$, $c = 15.090$	0.619
$Ti_3CoFe_4B_2$	$a = b = 8.619$, $c = 14.496$	0.408
$Ti_3Fe_5B_2$	$a = b = 8.624$, $c = 14.486$	0.251

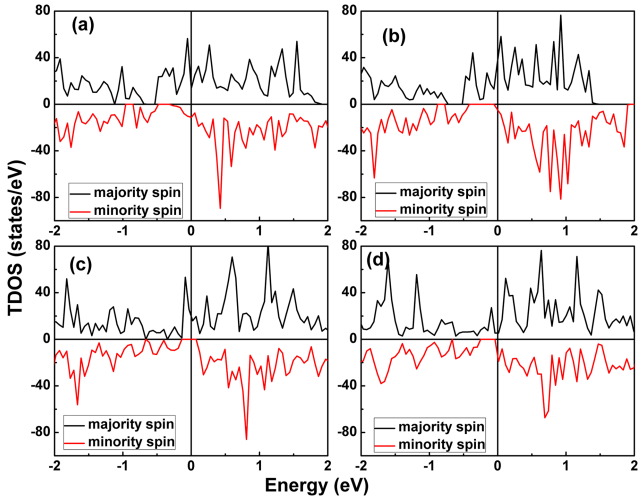

FIG. 3. Total densities of state for the thin films, which are all ferromagnetic: (a) $Ti_3Co_5B_2$, (b) $Ti_3Co_4FeB_2$, (c) $Ti_3CoFe_4B_2$, and (d)$Ti_3Fe_5B_2$.

The second part of our thin-film investigation is devoted to the calculation of the magnetocrystalline anisotropy. The microscopic origin of magnetocrystalline anisotropy is the spin-orbit coupling of the electrons in magnetic materials.[26] We have used the relation $K_1 = (E_x - E_z)/V$ to calculate the anisotropy constant, where V is the unit-cell volume and E_x and E_z are the ground-state energies when all spins are aligned in the x- and z-direction, respectively. Our calculations show that all members of the thin-film series have perpendicular magnetic anisotropy (PMA, $K_1 > 0$). In other words, the z-axis in Fig. 1 is the easy axis. Table III lists the values of K_1 for all thin films.

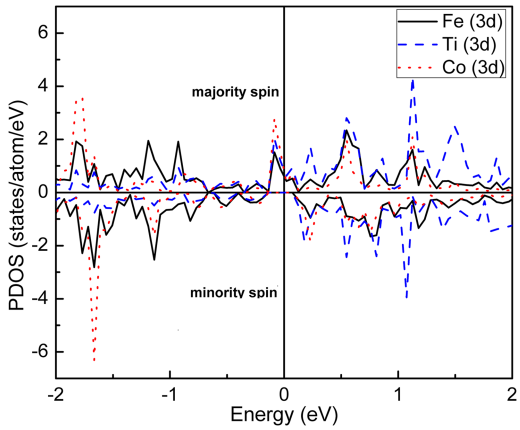

FIG. 4. Partial density of states for thin-film $Ti_3CoFe_4B_2$.

TABLE III. First anisotropy constants K_1 for the thin films.

Compound	$Ti_3Co_5B_2$	$Ti_3Co_4FeB_2$	$Ti_3CoFe_4B_2$	$Ti_3Fe_5B_2$
K_1 (MJ/m^3)	1.768	0.92	1.024	0.022

In Table III, we recognize the trend that the anisotropy decreases with decreasing Co content. Note that the combination of half-metallicity and perpendicular magnetic anisotropy in $Ti_3CoFe_4B_2$ is favorable for spintronics applications.[27]

IV. CONCLUSIONS

In summary, we have used first-principle density-functional theory to investigate $Ti_3Co_5B_2$, $Ti_3Co_4FeB_2$, $Ti_3CoFe_4B_2$ and $Ti_3Fe_5B_2$ in both bulk and thin-film form. Our bulk calculations show that only one member of the bulk series is ferromagnetic, namely $Ti_3Fe_5B_2$ that where all Co atoms are replaced by Fe, the other bulk compounds are Pauli-paramagnetic. By contrast, all thin-film alloys are ferromagnetic and exhibit easy-axis magnetocrystalline anisotropy. One member of the thin-film series, namely $Ti_3CoFe_4B_2$, is half-metallic in addition to having easy-axis anisotropy, which makes it a potential candidate for spintronics applications.

ACKNOWLEDGMENTS

This work is supported by Nano Mission, DST, India (R. P., I. A., A. K) and by the DOE-EERE-VT-EDT program under the DREaM project at the Ames Laboratory (DE-AC02-07CH11358, W.-Y. Zh., R. S., D. J. S.), and NCMN (Sh. V.).

[1] Y. B. Kuz'ma and Y. P. Yarmolyuk, "Crystal structure of the compound $Ti_3Co_5B_2$," J. Struct. Chem. **12**(3), 422–424.
[2] W. Y. Zhang, R. Skomski, A. Kashyap, S. Valloppilly, X. Z. Li, J. E. Shield, and D. J. Sellmyer, "Coercivity and nanostructure of melt-spun Ti-Fe-Co-B-based alloys," AIP Adv. **6**(5), 56001 (2016).
[3] R. W. McCallum, L. H. Lewis, R. Skomski, M. J. Kramer, and I. E. Anderson, "Practical aspects of modern and future permanent magnets," Annu. Rev. Mater. Res. **44**(1), 451–477 (2014).
[4] R. Skomski, P. Manchanda, P. Kumar, B. Balamurugan, A. Kashyap, and D. J. Sellmyer, "Predicting the future of permanent-magnet materials," IEEE Trans. Magn. **49**(7), 3215–3220 (2013).
[5] K. Ando, S. Fujita, J. Ito, S. Yuasa, Y. Suzuki, Y. Nakatani, T. Miyazaki, and H. Yoda, "Spin-transfer torque magnetoresistive random-access memory technologies for normally off computing (invited)," J. Appl. Phys. **115**(17), 172607 (2014).
[6] R. Courtland, "Spin memory shows its might [News]," IEEE Spectr. **51**(8), 15–16 (2014).
[7] S. A. Wolf, D. D. Awschalom, R. A. Buhrman, J. M. Daughton, S. von Molnár, M. L. Roukes, A. Y. Chtchelkanova, and D. M. Treger, "Spintronics: A spin-based electronics vision for the future," Science **294**(5546), 1488–1495 (2001).
[8] A. D. Kent and D. C. Worledge, "A new spin on magnetic memories," Nat. Nanotechnol. **10**(3), 187–191 (2015).
[9] R. A. de Groot, F. M. Mueller, P. G. van Engen, and K. H. J. Buschow, "New class of materials: Half-metallic ferromagnets," Phys. Rev. Lett. **50**(25), 2024–2027 (1983).
[10] T. Graf, C. Felser, and S. S. P. Parkin, "Simple rules for the understanding of Heusler compounds," Prog. Solid State Chem. **39**(1), 1–50 (2011).
[11] P. J. Webster, "Heusler alloys," Contemp. Phys. **10**(6), 559–577 (1969).
[12] T. Block, M. J. Carey, B. A. Gurney, and O. Jepsen, "Band-structure calculations of the half-metallic ferromagnetism and structural stability of full- and half-Heusler phases," Phys. Rev. B **70**(20), 205114 (2004).
[13] D. P. Oxley, R. S. Tebble, and K. C. Williams, "Heusler alloys," J. Appl. Phys. **34**(4), 1362–1364 (1963).
[14] A. J. Bradley and J. W. Rodgers, "The crystal structure of the Heusler alloys," Proc. R. Soc. Lond. Math. Phys. Eng. Sci. **144**(852), 340–359 (1934).
[15] H. Akinaga, T. Manago, and M. Shirai, "Material design of half-metallic Zinc-Blende CrAs and the synthesis by molecular-beam pitaxy," Jpn. J. Appl. Phys. **39**(no. Part 2, No. 11B), L1118–L1120 (2000).
[16] Y. Okimoto, T. Katsufuji, T. Ishikawa, A. Urushibara, T. Arima, and Y. Tokura, "Anomalous variation of optical spectra with spin polarization in double-exchange ferromagnet: $La_{1-x}Sr_xMnO_3$," Phys. Rev. Lett. **75**(1), 109–112 (1995).
[17] K. Schwarz, "CrO_2 predicted as a half-metallic ferromagnet," J. Phys. F Met. Phys. **16**(9), L211 (1986).
[18] V. Alijani, J. Winterlik, G. H. Fecher, S. S. Naghavi, and C. Felser, "Quaternary half-metallic Heusler ferromagnets for spintronics applications," Phys. Rev. B **83**(18), 184428 (2011).
[19] J. Winterlik, S. Chadov, A. Gupta, V. Alijani, T. Gasi, K. Filsinger, B. Balke, G. H. Fecher, C. A. Jenkins, F. Casper, J. Kübler, G.-D. Liu, L. Gao, S. S. P. Parkin, and C. Felser, "Design scheme of new tetragonal Heusler compounds for spin-transfer torque applications and its experimental realization," Adv. Mater. **24**(47), 6283–6287 (2012).
[20] R. Sahoo, L. Wollmann, S. Selle, T. Höche, B. Ernst, A. Kalache, C. Shekhar, N. Kumar, S. Chadov, C. Felser, S. S. P. Parkin, and A. K. Nayak, "Compensated ferrimagnetic tetragonal Heusler thin films for antiferromagnetic spintronics," Adv. Mater., n/a-n/a (2016).

[21] Q. Ma, A. Sugihara, K. Suzuki, X. Zhang, T. Miyazaki, and S. Mizukami, "Tetragonal Heusler-like Mn–Ga alloys based perpendicular magnetic tunnel junction," SPIN **4**(4), 1440024 (2014).
[22] J. P. Perdew, K. Burke, and M. Ernzerhof, "Generalized gradient approximation made simple," Phys. Rev. Lett. **77**(18), 3865–3868 (1996).
[23] G. Kresse and D. Joubert, "From ultrasoft pseudopotentials to the projector augmented-wave method," Phys. Rev. B **59**(3), 1758–1775 (1999).
[24] G. Kresse and J. Furthmüller, "Efficiency of ab-initio total energy calculations for metals and semiconductors using a plane-wave basis set," Comput. Mater. Sci. **6**(1), 15–50 (1996).
[25] M. Methfessel and A. T. Paxton, "High-precision sampling for Brillouin-zone integration in metals," Phys. Rev. B **40**(6), 3616–3621 (1989).
[26] R. Skomski and J. M. D. Coey, *Permanent magnetism* (Institute of Physics, Bristol, 1999).
[27] Z. Bai, L. Shen, G. Han, and Y. P. Feng, "Data storage: Review of heusler compounds," SPIN **2**(4), 1230006 (2012).